

# Electrically controlled persistent spin currents at the interface of multiferroic oxides

Chenglong Jia and Jamal Berakdar

*Institut für Physik, Martin-Luther Universität Halle-Wittenberg, 06120 Halle (Saale), Germany*

(Received 10 June 2009; revised manuscript received 2 July 2009; published 29 July 2009)

We predict the appearance of a persistent spin current in a two-dimensional electron gas formed at the interface of multiferroic oxides with a transverse helical magnetic order. No charge current is generated. This is the result of an effective spin-orbit coupling generated by the topology of the oxide local magnetic moments. The effective coupling and the generated spin current depend linearly on the magnetic spiral helicity which, due to the magnetoelectric coupling, is tunable by a transverse electric-field offering thus a new mean for the generation of electrically controlled persistent spin currents.

DOI: [10.1103/PhysRevB.80.014432](https://doi.org/10.1103/PhysRevB.80.014432)

PACS number(s): 72.25.-b, 68.47.Gh, 73.20.-r, 85.75.-d

## I. INTRODUCTION

Nanoscience research is fueled by the spectacular functionalities that emerge from the controlled composition of different materials down to the atomic level. A recent example is the appearance of a metallic phase with a high carrier mobility confined to the interface between insulating oxides<sup>1</sup> such as  $\text{LaTiO}_3/\text{SrTiO}_3$  or  $\text{LaAlO}_3/\text{SrTiO}_3$ .<sup>2</sup> This sheet of two-dimensional electron gas (2DEG) has been laterally confined and patterned<sup>3</sup> to achieve nanometer-sized tunnel junctions and field-effect transistors,<sup>4</sup> thus paving the way for oxide-based nanoelectronics<sup>3</sup> with a multitude of technological applications.<sup>5</sup> Further functionalities are expected when utilizing the residual properties of the oxides. For example, an important group of Mott insulating oxides such as  $\text{RMnO}_3$  ( $R=\text{Tb, Dy, Gd, and Eu}_{1-x}\text{Y}_x$ )<sup>6</sup> and  $\text{LiCu}_2\text{O}_2$  (Ref. 7) are multiferroics with a noncollinear magnetic phase. The origin of the spontaneous electric polarization is argued<sup>8</sup> to be the spin current associated with the spiral magnetic order. As shown experimentally, due to the magnetoelectric coupling, the helicity associated with the spin spiral structure of the multiferroics is tunable from clockwise to counterclockwise type by a small electric field ( $\sim 1$  kV/cm).<sup>9</sup>

In this paper we show theoretically, that a 2DEG formed at the surface of a multiferroic oxide (Fig. 1) such as the  $ab$  plane of  $\text{TbMnO}_3$  (Ref. 6) experiences an effective spin-orbit interaction (SOI) that linearly depends on the carriers wave vector and on the helicity of the oxide's magnetic order and hence is controllable by a lateral electric field. As a result an electrically tunable *persistent spin current* is shown to buildup in the 2DEG. No charge current is generated. The origin of this effect lies in the topological structure of the local magnetic moment at the oxides interface. Spin currents are actively discussed in the field of semiconductor-based spintronics.<sup>10-14</sup> There, SOI plays also a vital role. In semiconductors, however, a finite dissipative charge current is also generated by the applied in-plane electric field. Hence, the persistent spin current in insulator,<sup>15</sup> as uncovered here, has a decisive advantage, as compared with metals<sup>16</sup> and semiconductors<sup>12</sup> and adds a new twist to oxide electronics.

## II. THEORETICAL FORMULATION

As sketched in Fig. 1, we consider a 2DEG, as realized in Refs. 1-4 at the interfaces of oxides layers, however, one of

the layers should be a spiral multiferroic oxide such as  $\text{TbMnO}_3$  (Ref. 6) or  $\text{LiCu}_2\text{O}_2$ .<sup>7</sup> The spiral structure defines the  $x$ - $z$  plane, whereas the 2DEG is confined to the  $x$ - $y$  plane (cf. Fig. 1). At low temperature, the oxide local spin dynamics is much slower than the 2DEG carrier dynamics and hence we can treat the oxide local moments as classical and static. A carrier in the 2DEG with a charge  $e$  experiences an effective (real) internal magnetic field due to the magnetic spiral and the embedding medium<sup>17-19</sup> which results in a nonlocal vector potential  $\mathbf{A}_{in}$ . The effect of  $\mathbf{A}_{in}$  on the charge carriers dynamics is subsidiary compared to that of the exchange field  $J\mathbf{n}_r$ , where  $\mathbf{n}_r$  is a local unit-vector field describing the geometry of the localized magnetic moments at the oxides interface and  $J$  is the coupling strength. The exchange interaction originates from the Coulomb repulsion at the sites of the localized moments and from the Hund's rule coupling in the magnetically ordered phase.<sup>8,20,21</sup> Thus, the single-particle dynamics in the 2DEG is governed by the Hamiltonian<sup>5</sup>

$$H = h_k + h_J = \frac{1}{2m}\mathbf{P}^2 + J\mathbf{n}_r \cdot \boldsymbol{\sigma}, \quad (1)$$

where  $m$  is the effective electron mass,  $\boldsymbol{\sigma}$  is the vector of the Pauli matrices, and  $\mathbf{P}$  is the momentum operator.  $\mathbf{n}_r$  is given by the local magnetization at the multiferroic surface, i.e.,  $\mathbf{n}_r = (\sin \theta_r, 0, \cos \theta_r)$ , where  $\theta_r = \mathbf{q}_m \cdot \mathbf{r}$  with  $\mathbf{q}_m = (q, 0, 0)$  being the spin wave vector of the spiral.  $\mathbf{A}_{in}$  is not included in Eq. (1).<sup>22</sup>

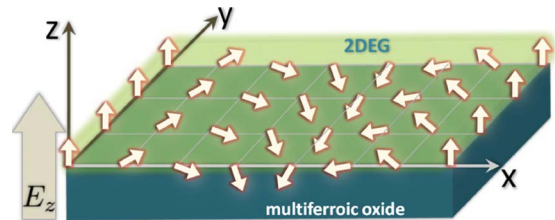


FIG. 1. (Color online) Schematics of the proposed system. The  $x$  axis is defined along the direction of the spiral ordering, for example, the  $[110]$  direction in  $\text{TbMnO}_3$ . The spiral plane of multiferroic (below) is perpendicular to the 2DEG (above). Due to magnetoelectric coupling the spin helicity is controlled by the transverse electric field  $E_z$ .

Applying the unitary local gauge transformation in the spin space  $U_g = \exp(-i\theta_r \sigma_y / 2)$ , the spatially nonhomogeneous term  $h_J$  is transformed into the diagonal term<sup>24</sup>  $\tilde{h}_J = U_g^\dagger h_J U_g = J \tilde{\sigma}_z$  (Hereafter, transformed quantities are marked by a tilde). Physically, this amounts to a rotation of the local quantization axis to align with  $\mathbf{n}_r$  at each site.  $\sigma_y = \tilde{\sigma}_y$  because  $[U_g, \sigma_y] = 0$ . We find further  $\tilde{\sigma}_x = (\sigma_x \cos \theta_r - \sigma_z \sin \theta_r)$  and  $\tilde{\sigma}_z = (\sigma_x \sin \theta_r + \sigma_z \cos \theta_r)$ . The simplicity of  $\tilde{h}_J$  comes at the price of introducing an additional gauge field  $\mathbf{A}_g = -i\hbar U_g^\dagger \nabla_r U_g$  in the transformed kinetic energy  $\tilde{h}_k$ .<sup>25</sup> The gauge field  $\mathbf{A}_g$  depends only on the geometry of the local magnetization at the oxide interface. As shown below,  $\mathbf{A}_g$  acts as a  $q$  and momentum-dependent effective SOI that can be changed electrically because  $q$  is tunable by a transverse electric field, as shown in Fig. 1.

For clarity, we introduce the scaled variables (denoted by a bar)  $\bar{\mathbf{r}} = \mathbf{r}/a$ ,  $\bar{q} = aq$ , and  $\bar{\mathbf{k}} = a\mathbf{k}$ , where  $a$  is the lattice constant and  $\mathbf{k}$  is the crystal momentum. The scaled energy  $\bar{E}$ , and the scaled exchange energy  $\Delta_m$  read

$$\bar{E} = E/\epsilon_0, \quad \Delta_m = J/\epsilon_0 \quad \text{with} \quad \epsilon_0 = \frac{\hbar^2}{2ma^2}. \quad (2)$$

Then for the scaled Hamiltonian we find the expression

$$\bar{H} = \left[ \left( i\nabla_{\bar{x}} + \frac{\bar{q}}{2} \tilde{\sigma}_y \right)^2 + (i\nabla_{\bar{y}})^2 \right] + \Delta_m \tilde{\sigma}_z. \quad (3)$$

For a realistic estimate of the parameters of the 2DEG at oxides interfaces we choose the lattice constant  $a = 5 \text{ \AA}$ . To our knowledge, the effective mass  $m$  of 2DEG at oxide interface is not yet determined. For insulators, however,  $m$  is usually quite large, e.g., for  $\text{SrTiO}_3$   $m$  is  $\sim 100$  times larger than for  $\text{GaAs}$ .<sup>2</sup> Here we choose  $m/m_e = 10$  with  $m_e$  being the free-electron mass which sets the unit of energy to  $\epsilon_0 \approx 15 \text{ meV}$ . We can rewrite Hamiltonian (3) in the form<sup>26</sup>

$$\bar{H} = \bar{k}_x^2 + \bar{k}_y^2 + \bar{q} \bar{k}_x \tilde{\sigma}_y + \Delta_m \tilde{\sigma}_z. \quad (4)$$

This relation reveals the existence of a SOI that depends linearly on  $\bar{q}$  and  $\bar{\mathbf{k}}$ , for the collinear spin phase ( $\bar{q} \rightarrow 0$ ) this SOI vanishes. The dependence on  $\bar{k}_x$  resembles the case of a semiconductor 2DEG in a perpendicular magnetic field with the Rashba<sup>27</sup> and Dresselhaus<sup>28</sup> SOIs having equal strengths. In this case, when the magnetic-field vector potential is taken into account one obtains a resonant spin Hall conductance; the spin current is carried by a charge Hall conductivity.<sup>29</sup> Such a resonance behavior is present for a perpendicular spin polarization. In our oxide system, however, all averaged values of spin polarization vanish due to a zero average magnetization in the original spin basis.

Explicitly diagonalizing Hamiltonian (4) we obtain the eigenenergies

$$\bar{E}_\pm(\bar{\mathbf{k}}) = \bar{k}_x^2 + \bar{k}_y^2 \pm \sqrt{\Delta_m^2 + (\bar{q} \bar{k}_x)^2} \quad (5)$$

with the eigenstates

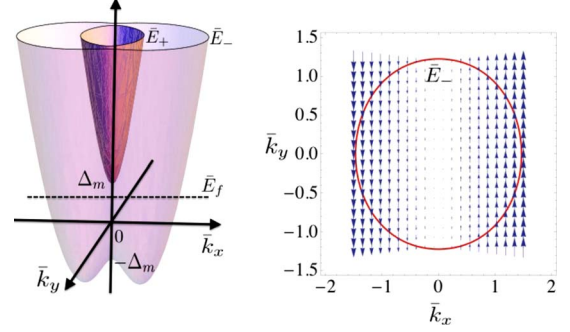


FIG. 2. (Color online) Energy bands: (left panel)  $\bar{E}_\pm$  corresponds to the two energy branches, respectively. When  $\bar{E}_f < \Delta_m$ , only the low-energy band  $\bar{E}_-$  is relevant for the Fermi contour (right panel). The arrows represent the effective SOI,  $\bar{q} \bar{k}_x \tilde{\sigma}_y$ . The strengths of the carrier coupling to the local magnetic order are chosen as  $\bar{E}_f/\Delta_m = 1/2$  and the spiral wave vector is  $\bar{q} = 2\pi/7$ .

$$|\psi_+\rangle = e^{-i\bar{\mathbf{k}} \cdot \bar{\mathbf{r}}} \begin{pmatrix} \cos \frac{\phi}{2} \\ i \sin \frac{\phi}{2} \end{pmatrix}, \quad |\psi_-\rangle = e^{-i\bar{\mathbf{k}} \cdot \bar{\mathbf{r}}} \begin{pmatrix} i \sin \frac{\phi}{2} \\ \cos \frac{\phi}{2} \end{pmatrix}, \quad (6)$$

where

$$\tan \phi = \frac{\bar{q} \bar{k}_x}{\Delta_m}, \quad \cos \phi = \frac{\Delta_m}{\sqrt{\Delta_m^2 + (\bar{q} \bar{k}_x)^2}}. \quad (7)$$

Due to the effective spin-orbit coupling, the Fermi contours are not parabolic but anisotropic having  $\hat{x}$  and  $\hat{y}$  as the symmetry axes, as depicted in Fig. 2. Although the spin states in Eq. (6) are not independent of  $\bar{\mathbf{k}}$ , we still have a disappearance of the Berry phase just as for the case without magnetic field in Ref. 30. Thus implies that a spin current along the spin  $\hat{z}$  direction does not exist in the absence or presence of an electric field.

### III. PERSISTENT SPIN CURRENT

The expectation value of the spin polarizations per electron evaluated using the eigenstates (6) are

$$\langle \tilde{\sigma}_y^s \rangle = \frac{s \bar{q} \bar{k}_x}{\sqrt{\Delta_m^2 + (\bar{q} \bar{k}_x)^2}} \quad (8)$$

$$\langle \tilde{\sigma}_z^s \rangle = \frac{s \Delta_m}{\sqrt{\Delta_m^2 + (\bar{q} \bar{k}_x)^2}}. \quad (9)$$

Here  $s = \pm$ , the double sign corresponds to the two branches of the energy dispersion Eq. (5). In the original spin space,  $\langle \tilde{\sigma}_z^s \rangle$  corresponds to a spiral spin ordering induced by the exchange interaction between the 2DEG and the local magnetic moments at the oxide surface. Obviously, the  $\hat{y}$  spin-polarization component  $\langle \sigma_y^s \rangle$  is odd in  $\bar{k}_x$  and hence it vanishes upon summation over all occupied states. The spin current in the  $\hat{x}$  direction is, however, generally *finite* when

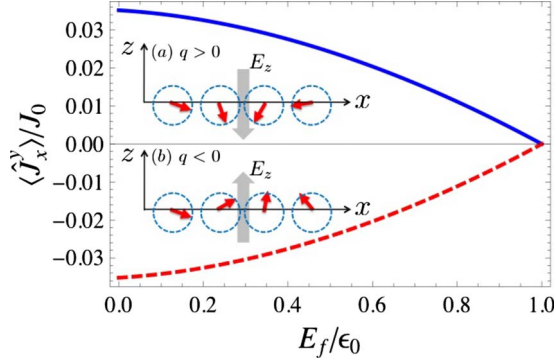


FIG. 3. (Color online) The persistent spin current as a function of  $E_f$  for positive (a) and negative (b) helicities when the Fermi level intersects only the low-energy band. The parameters are chosen as  $\epsilon_0 = 15$  meV,  $J_0 = a\epsilon_0/2$ ,  $\Delta_m = \epsilon_0$ , and  $\bar{q} = 2\pi/7$ . As illustrated in the insets, depending on the direction of an applied transverse electric field  $E_z$  the spiral helicity and hence the spin current directions are reversible due to the magnetoelectric coupling.

the Fermi level intersects only one of the two bands. To prove this we consider the spin current operator, defined as

$$\hat{J}_j^i = \frac{\hbar}{4} (\sigma_i v_j + v_j \sigma_i), \quad (10)$$

where the velocity operators at each  $\bar{\mathbf{k}}$  are given by  $v_x = \partial H / \partial p_x = \frac{\hbar}{2ma} (2\bar{k}_x + \bar{q}\bar{\sigma}_y)$  and  $v_y = \partial H / \partial p_y = \frac{\hbar\bar{k}_y}{ma}$ . Considering the symmetry  $\bar{E}_s(\bar{\mathbf{k}}) = \bar{E}_s(-\bar{\mathbf{k}})$  of the eigenenergies [Eq. (5)], it follows that only  $\langle \hat{J}_x^y \rangle$  is finite and is determined by (in unit of  $J_0 = \frac{\hbar^2}{4ma}$ )

$$\langle \hat{J}_x^y \rangle = \sum_{s=\pm} \int \frac{d^2\bar{\mathbf{k}}}{(2\pi)^2} (2\bar{k}_x \bar{\sigma}_y^s + \bar{q}) f[\bar{E}_s(\bar{\mathbf{k}})], \quad (11)$$

where  $f[\bar{E}_s(\bar{\mathbf{k}})]$  is the Fermi-Dirac distribution, and  $\bar{\mathbf{k}}$  runs over all occupied states. Introducing the wave-vector parameterization  $\bar{\mathbf{k}} = \bar{k}(\cos \varphi, \sin \varphi)$ , it can be analytically shown that  $\langle \hat{J}_x^y \rangle = 0$  when  $\bar{E}_f \geq \Delta_m$ . However, as shown in Fig. 3, the spin current is finite when only the low-energy band is intersected by the Fermi level. Interestingly, the spin current is related to the electron density,  $n_f$  through the Fermi energy  $E_f$ . More important, the key factor is the *odd* relationship between the spin current and the geometrical spiral structure of the magnetic ordering, being clockwise ( $\bar{q} < 0$ ) or anti-clockwise ( $\bar{q} > 0$ ) (Fig. 3). This is insofar important, as spin-polarized neutron scattering experiments<sup>9</sup> on multiferroics evidently show that the helicity of the spiral magnetic order is controllable by a small ( $\sim 1$  kV/cm) transverse electric field, as illustrated in Fig. 3.

In the absence of an electric field, when the exchange interaction is strong enough, i.e., for large  $\Delta_m$ , the spins of the conduction electrons are initially aligned locally parallel to  $\mathbf{n}_r$  at each site,  $\langle \bar{\sigma}_z \rangle = 1$ . Using the Heisenberg equation for the electron-spin motion,<sup>31</sup> we find in the linear response regime that the 2DEG develops a uniform spin polarization

$$\langle \bar{\sigma}_x \rangle = -\bar{q} \frac{eaE_x}{2\epsilon_0\Delta_m^2}, \quad (12)$$

when an external electric field is applied along  $\hat{x}$  direction. Transforming back reveals that the solution for  $\langle \bar{\sigma}_x \rangle$  corresponds to the emergence of a spiral spin-density wave in the 2DEG that rotates in the  $x$ - $z$  plane. The direction of the spin polarization is orthogonal to the oxide local magnetic moment. Furthermore, the linear dependence on  $q$  of  $\langle \bar{\sigma}_x \rangle$  allows for an electric-field control of the induced spin helicity.

#### IV. HALL CONDUCTIVITY

The oxide magnetic order is usually not exactly coplanar in the  $y$ - $z$  plane but it has a small deviation. Here we simulate this noncoplanar modulation with a slowly varying spiral order with a spin helicity given by  $(0, \beta\bar{q}, 0)$  ( $\beta \ll 1$ ) along  $\hat{y}$  direction. This results in another effective spin-orbit coupling term  $\sim \beta\bar{q}\bar{k}_y\bar{\sigma}_x$  with a strength  $\beta\bar{q}$ . In analogy to the semiconductor case, this amounts to the Rashba and the Dresselhaus SOIs having different strengths. Therefore, we expect in our case the existence of a Hall effect. To see this, we diagonalize the resulting total Hamiltonian using the transformation

$$T = \begin{pmatrix} \bar{q} \sin \frac{\phi'}{2} \begin{pmatrix} -\beta\bar{k}_y + i\bar{k}_x \\ F_{\bar{k}} \end{pmatrix} & \cos \frac{\phi'}{2} \\ \cos \frac{\phi'}{2} & \bar{q} \sin \frac{\phi'}{2} \begin{pmatrix} \beta\bar{k}_y + i\bar{k}_x \\ F_{\bar{k}} \end{pmatrix} \end{pmatrix}, \quad (13)$$

where

$$\cos \phi' = \frac{\Delta_m}{\sqrt{\Delta_m^2 + F_{\bar{k}}^2}}, \quad F_{\bar{k}} = \bar{q} \sqrt{\bar{k}_x^2 + \beta^2 \bar{k}_y^2}. \quad (14)$$

The Hall effect in the 2DEG is related to the nontrivial topology of the resulting eigenstates  $|\bar{k}\rangle$  in the momentum space,<sup>11,19,32</sup> expressed through the gauge connection  $\mathcal{A}_{\bar{k}} = -i\langle \bar{k} | \nabla_{\bar{k}} | \bar{k} \rangle$ . The off-diagonal Hall conductivity is related to Berry's curvature<sup>11</sup>  $\Omega_s^z = \nabla_{\bar{k}} \times \mathcal{A}_{\bar{k}}$  pointing along the  $\hat{z}$  axis, for which we obtain

$$\Omega_s^z = -\frac{s}{2} \frac{\beta}{\cos^2 \varphi + \beta^2 \sin^2 \varphi} \frac{1}{\bar{k}} \frac{\partial \cos \phi'}{\partial \bar{k}}. \quad (15)$$

$\Omega_s^z$  diverges along the  $\hat{y}$  axis at very small  $\beta$ , and is singular at the origin  $\bar{k} = 0$ . The geometrical Berry phase factor  $\gamma_s$  is given by the integral of the curvature over all wave vector

$$\gamma_s = \int \Omega_s^z d^2\bar{\mathbf{k}} = s\pi [1 - I(\beta, \bar{k}_s^2)], \quad (16)$$

$$I(\beta, \bar{k}_s^f) = \frac{1}{2\pi} \int_0^{2\pi} \frac{\beta}{\cos^2 \varphi + \beta^2 \sin^2 \varphi} \frac{\Delta_m}{\sqrt{\Delta_m^2 + F_{\bar{k}_s^f}^2}}. \quad (17)$$

The Fermi wave vector  $\bar{k}_s^f$  is given by the Fermi energy  $\bar{E}_f = \bar{k}^2 \pm \sqrt{\Delta_m^2 + F_{\bar{k}_s^f}^2}$ . At zero temperature, the off-diagonal Hall conductivity  $\sigma_{xy}$  for a full band is equal to the integral over the Brillouin zone of the component of the Berry curvature parallel to  $\hat{z}$  and is thus proportional to the Berry phase,<sup>11,19</sup> i.e.,

$$\sigma_{xy}^s = \frac{e^2}{\hbar} \int \Omega_s^z \frac{d^2 \bar{\mathbf{k}}}{(2\pi)^2} = s \frac{e^2}{2h} [1 - I(\beta, \bar{k}_s^f)]. \quad (18)$$

For a small  $\beta$ ,  $I(\beta, \bar{k}_s^f) \rightarrow 0$  and  $\sigma_{xy} = -\frac{e^2}{2h}$  is quantized when only one of the two bands intersects the Fermi level. Generally,  $\sigma_{xy}$  is not quantized, but the transverse conductivity should still be observable.

## V. SUMMARIZING

A persistent spin current emerges in 2DEG at the interface of a helimagnet due to the spiral geometry of the local magnetic order. The spin current is an odd function of the spin

helicity and hence electrically controllable by a small transverse electric field that reverses the spin helicity, making thus a link between spintronics and oxide electronics. For an in-plane electric field along the spiral we predict the buildup of a carrier spiral spin density wave. The spin Berry phase induced by a chiral magnetic texture in a Kagomé lattice has been discussed in Ref. 20. Due to a nonzero spin chirality defined as the mixed product of three spins on a certain plaquette,  $\chi_{ijk} = \mathbf{S}_i \cdot (\mathbf{S}_j \times \mathbf{S}_k)$ , they showed that the Berry phase contribution to the Hall conductivity is quantized for some values of the band filling (note, in our Fig. 1  $\chi_{ijk} = 0$ ). We also calculated the Berry curvature and obtained a finite Hall conductivity for even a small derivation from the coplanar oxide helical magnetic order. The transverse conductivity is determined by the chirality ( $\beta$ ), the electron density ( $\bar{k}_s^f$ ), and the strength of the exchange interaction ( $\Delta_m$ ),  $\sigma_{xy}$  can thus be quantized, or possesses a nonmonotonic behavior upon varying the relevant parameters.

## ACKNOWLEDGMENT

This research is supported by the DFG (Germany) through the project-B7 in the SFB762: *functionality of oxide interfaces*.

- 
- <sup>1</sup>A. Ohtomo and H. Y. Hwang, Nature (London) **427**, 423 (2004); **441**, 120 (2006); A. Ohtomo, D. A. Muller, J. L. Grazul, and H. Y. Hwang, *ibid.* **419**, 378 (2002).
- <sup>2</sup>S. Thiel, G. Hammerl, A. Schmehl, C. W. Schneider, and J. Mannhart, Science **313**, 1942 (2006); J. Mannhart, D. H. A. Blank, H. Y. Hwang, A. J. Millis, and J.-M. Triscone, MRS Bull. **33**, 1027 (2008).
- <sup>3</sup>C. Cen, S. Thiel, J. Mannhart, and J. Levy, Science **323**, 1026 (2009).
- <sup>4</sup>C. H. Ahn, J.-M. Triscone, and J. Mannhart, Nature (London) **424**, 1015 (2003).
- <sup>5</sup>C. Jia and J. Berakdar, Appl. Phys. Lett. **95**, 012105 (2009).
- <sup>6</sup>T. Kimura, T. Goto, H. Shintani, K. Ishizaka, T. Arima, and Y. Tokura, Nature (London) **426**, 55 (2003); T. Goto, T. Kimura, G. Lawes, A. P. Ramirez, and Y. Tokura, Phys. Rev. Lett. **92**, 257201 (2004); M. Kenzelmann, A. B. Harris, S. Jonas, C. Broholm, J. Schefer, S. B. Kim, C. L. Zhang, S.-W. Cheong, O. P. Vajk, and J. W. Lynn, *ibid.* **95**, 087206 (2005); Y. Yamasaki, S. Miyasaka, Y. Kaneko, J.-P. He, T. Arima, and Y. Tokura, *ibid.* **96**, 207204 (2006); J. Hemberger, F. Schrettle, A. Pimenov, P. Lunkenheimer, V. Yu. Ivanov, A. A. Mukhin, A. M. Balbashov, and A. Loidl, Phys. Rev. B **75**, 035118 (2007).
- <sup>7</sup>S. Park, Y. J. Choi, C. L. Zhang, and S.-W. Cheong, Phys. Rev. Lett. **98**, 057601 (2007).
- <sup>8</sup>H. Katsura, N. Nagaosa, and A. V. Balatsky, Phys. Rev. Lett. **95**, 057205 (2005); I. A. Sergienko and E. Dagotto, Phys. Rev. B **73**, 094434 (2006); C. Jia, S. Onoda, N. Nagaosa, and J.-H. Han, *ibid.* **76**, 144424 (2007).
- <sup>9</sup>Y. Yamasaki, H. Sagayama, T. Goto, M. Matsuura, K. Hirota, T. Arima, and Y. Tokura, Phys. Rev. Lett. **98**, 147204 (2007); S. Seki, Y. Yamasaki, M. Soda, M. Matsuura, K. Hirota, and Y. Tokura, *ibid.* **100**, 127201 (2008).
- <sup>10</sup>N. Nagaosa, J. Phys. Soc. Jpn. **77**, 031010 (2008).
- <sup>11</sup>D. Culcer, A. MacDonald, and Q. Niu, Phys. Rev. B **68**, 045327 (2003); P. Bruno, arXiv:cond-mat/0506270 (unpublished).
- <sup>12</sup>Y. Kato, R. C. Myers, A. C. Gossard, and D. D. Awschalom, Nature (London) **427**, 50 (2004); J. Wunderlich, B. Kaestner, J. Sinova, and T. Jungwirth, Phys. Rev. Lett. **94**, 047204 (2005).
- <sup>13</sup>S. Murakami, N. Nagaosa, and S.-C. Zhang, Science **301**, 1348 (2003); J. Sinova, D. Culcer, Q. Niu, N. A. Sinitsyn, T. Jungwirth, and A. H. MacDonald, Phys. Rev. Lett. **92**, 126603 (2004).
- <sup>14</sup>M. I. Dyakonov and V. I. Perel, Sov. Phys. JETP **13**, 467 (1971); J. E. Hirsch, Phys. Rev. Lett. **83**, 1834 (1999).
- <sup>15</sup>S. Murakami, N. Nagaosa, and S.-C. Zhang, Phys. Rev. Lett. **93**, 156804 (2004).
- <sup>16</sup>S. O. Valenzuela and M. Tinkham, Nature (London) **442**, 176 (2006); T. Kimura, Y. Otani, T. Sato, S. Takahashi, and S. Maekawa, Phys. Rev. Lett. **98**, 156601 (2007).
- <sup>17</sup>W. F. G. Swann, Phys. Rev. **49**, 574 (1936).
- <sup>18</sup>G. H. Wannier, Phys. Rev. **72**, 304 (1947).
- <sup>19</sup>R. Karplus and J. M. Luttinger, Phys. Rev. **95**, 1154 (1954).
- <sup>20</sup>K. Ohgushi, S. Murakami, and N. Nagaosa, Phys. Rev. B **62**, R6065 (2000); M. Taillefumier, B. Canals, C. Lacroix, V. K. Dugaev, and P. Bruno, *ibid.* **74**, 085105 (2006).
- <sup>21</sup>G. Tatara and H. Kawamura, J. Phys. Soc. Jpn. **71**, 2613 (2002); H. Kawamura, Phys. Rev. Lett. **90**, 047202 (2003).
- <sup>22</sup>Generally the determination of  $\mathbf{A}_{in}$  is quite involved and is geometry dependent. For an order of magnitude estimate we consider the contribution from the local magnetic moments, Ref. 23. The  $z$  component of the resulting  $\mathbf{H}$  field reads  $H_z(r) = \frac{1}{4\pi} \int d\mathbf{r}' \frac{\rho_m(r')(z-z')}{|\mathbf{r}-\mathbf{r}'|^3} \approx H_0 \cos qx$ ,  $H_0 = -\frac{1}{4\pi} \int d\mathbf{r}' \frac{z' \rho_m(r')}{|\mathbf{r}'|^3}$ ,  $\rho_m(r)$

$= -\nabla \cdot \mathbf{M}_{in}(r)$ , where  $\mathbf{M}_{in}$  is the oxide local magnetization,  $\mathbf{M}_{in} = (-1)^n M_0 \mathbf{n}_r$ . We thus have  $B_z(r) = \mu_0 [H_z(r) + M_z(r)] = B_0 \cos qx$ . In the Landau gauge the vector potential is space periodic, i.e.,  $\mathbf{A}_{in} = B_0(0, \frac{\sin qx}{q}, 0)$ .  $\mathbf{A}_{in}$  induces a periodic potential along the  $\hat{x}$  direction with an amplitude  $\frac{eB_0 a^2}{\hbar q}$  ( $a$  is the lattice constant), which is tiny in our case (the local magnetic moment is  $\approx 4\mu_B$  on each Mn site in  $RMnO_3$ , Ref. 6, the magnetic field is estimated as  $B_0 \sim 0.3$  T). The energy associated with the generated harmonic potential is  $\hbar e |B_z| / m = |B_z| \frac{m_e}{m} \times 10^{-1}$  meV with  $m_e$  being the free-electron mass. The effective mass  $m$  for the 2DEG at the oxide interfaces is  $m_e / m \sim 1/10$ , meaning a small energy contribution from the vector potential.

- <sup>23</sup>I. S. Ibrahim and F. M. Peeters, Phys. Rev. B **52**, 17321 (1995).  
<sup>24</sup>V. Korenman, J. L. Murray, and R. E. Prange, Phys. Rev. B **16**,

4032 (1977).

- <sup>25</sup>G. Tataru and H. Fukuyama, J. Phys. Soc. Jpn. **63**, 2538 (1994); P. Bruno, V. K. Dugaev, and M. Taillefumier, Phys. Rev. Lett. **93**, 096806 (2004).  
<sup>26</sup>A uniform energy displacement  $\Delta E = \bar{q}^2/4$  is disregarded in  $\bar{H}$ .  
<sup>27</sup>Y. A. Bychkov and E. I. Rashba, J. Phys. C **17**, 6039 (1984).  
<sup>28</sup>G. Dresselhaus, Phys. Rev. **100**, 580 (1955).  
<sup>29</sup>D. Zhang, Y.-M. Mu, and C. S. Ting, Appl. Phys. Lett. **92**, 212103 (2008); P. Lucignano, R. Raimondi, and A. Tagliacozzo, Phys. Rev. B **78**, 035336 (2008).  
<sup>30</sup>S.-Q. Shen, Phys. Rev. B **70**, 081311(R) (2004).  
<sup>31</sup>Y. Aharonov and A. Stern, Phys. Rev. Lett. **69**, 3593 (1992).  
<sup>32</sup>F. D. M. Haldane, Phys. Rev. Lett. **61**, 2015 (1988).